Polymer 50 (2009) 201–210

Contents lists available at ScienceDirect

Polymer

journal homepage: www.elsevier.com/locate/polymer

Novel role of polymer–solvent and clay–solvent interaction parameters on the thermal, mechanical and optical properties of polymer nanocomposites

Anusuya Choudhury [a], Anil K. Bhowmick [a,*], Christopher Ong [b]

[a] Rubber Technology Centre, Indian Institute of Technology Kharagpur, Kharagpur 721302, West Bengal, India
[b] LANXESS Deutschland GmbH, 41538 Dormagen, Germany

ARTICLE INFO

Article history:
Received 24 June 2008
Received in revised form
23 October 2008
Accepted 24 October 2008
Available online 6 November 2008

Keywords:
Hydrogenated nitrile rubber
Sepiolite
Interaction parameter

ABSTRACT

Solvent–polymer and solvent–clay interactions are very important in determining the properties of polymer–clay nanocomposites. In the present work, hydrogenated nitrile rubber–sepiolite nanocomposites were prepared and the interaction parameters of various solvents with rubber (χ_{AB}) and clay (χ_{CD}) were studied. Nine different sets of solvent combination were chosen based on their solubility parameter. A correlation between thermal, mechanical and optical transmittance properties of polymer–clay nanocomposites and the difference in their interaction parameters with various solvents ($\chi_{AB} - \chi_{CD}$) was analyzed for the first time. This study helped to identify chloroform/methyl ethyl ketone as the best solvent combination, where temperature at which maximum degradation of the polymer took place was raised by 65 °C and tensile strength and modulus at 100% elongation were enhanced by almost 200% over the neat rubber. The results were correlated with the data of X-Ray Diffraction study, Atomic Force Microscopy and Transmission Electron Microscopy. Finally, thermodynamic interpretation was made to explain the results.

1. Introduction

Polymer nanocomposites can be prepared mainly by three techniques, viz., in situ polymerization, solution mixing and melt mixing. In melt mixing, fillers are added directly into the polymer matrix, while solution mixing involves dispersion of the filler in an organic solvent followed by dissolution of the polymer matrix and solvent casting. It has been observed from earlier studies that solution mixing brings about better exfoliation/delamination and dispersion of nanoparticles in a polymer [1,2]. Thus, in solution mixing, solvent plays an important role in determining the properties of polymer–filler nanocomposites. Both the solvents might be either same or of different types, where the polymer gets dissolved in one solvent and the filler particles are dispersed in the other. Full dispersion of clay particles in a polymer is thus a major challenge.

There are many reports describing the preparation of polymer nanocomposites by solution mixing [1–6]. But none of these papers deal with importance of solvent in dispersion of clay in a matrix. Ho and Glinka [7] in their work have highlighted the effect of solvent solubility parameter on the dispersion of clay. Liu et al. [8] also have done similar work using single wall carbon nanotube. Lift et al. [9] have used a solvent exchange process for the proper dispersion of nanoparticles in thermoplastic elastomers. Lim et al. [10] measured the Flory–Huggins interaction parameter to determine the extent of miscibility between the blend of poly(ethylene oxide) and poly(methyl methacrylate) with organically modified montmorillonite clay. But no study has been done yet, which considers both the solvents for polymer and clay. Also, all the above studies have given emphasis on dispersion of clay in solvent or polymer matrix, but these studies do not show the effect of solvent on the dispersion as well as the properties of polymer–clay nanocomposites. Moreover, most of the earlier studies have been done on montmorillonite clay. Present work illustrates how the choice of a proper solvent system and the difference in interaction parameters of solvent and polymer (here, hydrogenated nitrile butadiene rubber, HNBR), and solvent and clay (here, sepiolite) affects the thermal, mechanical and optical properties, and thus this study fills the gap in the literature. There is also no literature on HNBR–sepiolite nanocomposite.

Hydrogenated nitrile butadiene rubber (HNBR), a special class of nitrile rubber (NBR) that is hydrogenated to increase the saturation of the hydrocarbon polymer backbone, has been chosen in the present study. This elastomer is known for its physical strength and retention of properties after long-term exposure to heat, oil and chemicals. However, there are some aggressive applications like hood hoses where much higher heat resistance is required and application of nanocomposite may be interesting.

* Corresponding author. Tel.: +91 3222 283180; fax: +91 3222 220312.
E-mail address: anilkb@rtc.iitkgp.ernet.in (A.K. Bhowmick).

0032-3861/$ – see front matter © 2008 Elsevier Ltd. All rights reserved.
doi:10.1016/j.polymer.2008.10.044

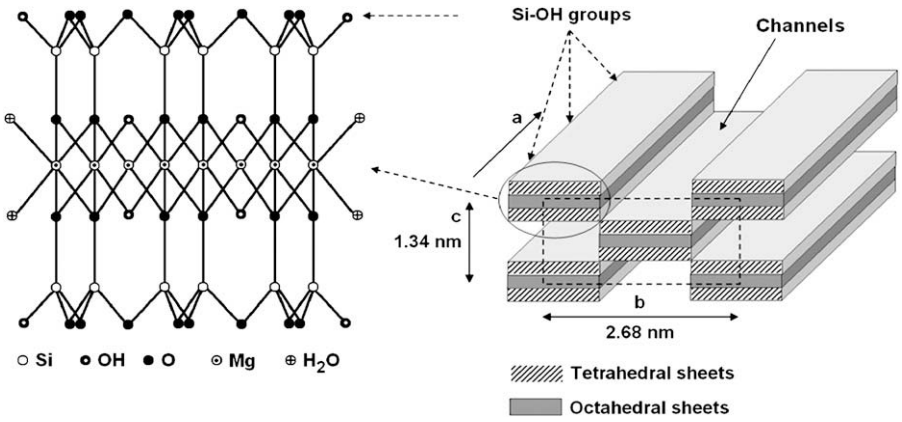

Fig. 1. Structure of sepiolite.

Sepiolite is a 2:1 phyllosilicate where one octahedral sheet is sandwiched between two tetrahedral sheets. But it is a hydrated magnesium silicate having chain structure and fibrous morphology. The tetrahedral sheets are extended to a considerable distance in the "*a*" and "*b*" directions (Fig. 1). However, at periodic intervals along the *b*-axis, the tetrahedral sheets invert and hence sepiolite is also called an "inverted ribbon." It contains fine micropore channels of dimension $0.37 \times 1.06\ nm^2$ running parallel to the length of the fiber [11]. Sepiolite, because of its fibrous morphology, high aspect ratio and presence of high density of silanol group, is expected to have a good interaction with polar groups of the polymer chain and is thus chosen in this investigation.

Understanding the interaction between clays and organic solvent as well as subsequent interaction of such an organoclay with polymer matrix dissolved in another solvent is a critical step towards determining the properties of nanocomposites. The improved properties are related to the degree of dispersion and extent of interaction of clay particles with polymer matrix.

Motivation of this work is to explore the correlation between interaction parameter of rubber–solvent and clay–solvent with properties of HNBR–sepiolite nanocomposites. For this purpose, HNBR–sepiolite nanocomposites have been prepared using nine different solvent combinations with varying solubility parameter (δ) (Table 1a). The dispersion of clay in the rubber matrix for different solvent systems has been characterized by X-Ray Diffraction, Atomic Force Microscopy and Transmission Electron Microscopy. Thermal, mechanical and optical properties of the nanocomposites prepared in various solvent combinations have been measured and finally an attempt has been made to correlate these properties with the interaction parameter of rubber–solvent and clay–solvent system. The results are further explained with the help of thermodynamics.

2. Experimental

2.1. Materials

Therban C3467, having acrylonitrile content = 34%, diene content = 5.5%, Mooney Viscosity, ML(1 + 4) at 100 °C = 68, specific gravity = 0.95, was obtained from Lanxess, Germany. Sepiolite Pangel B20 was kindly gifted by Tolsa S.A., Empres, Mercedes, Spain. Pangel B20 is treated with an organic material, quaternary ammonium salt such as dimethylbenzylalkylammonium chloride, to make the clay more "organophilic," i.e., more compatible with systems of low-to-medium polarity. This was obtained from pristine sepiolite by means of specific physico-chemical purification, micronization and chemical modification processes. The micronization leads to a disagglomeration of the bundles of microfibres [12]. Solvents used in this study were supplied by Merck Limited, Mumbai. Tables 1a and 1b report the details of the solvents and combination of solvents used in this study.

2.2. Preparation of hydrogenated nitrile rubber (HNBR)–sepiolite nanocomposites

The rubber was first dissolved in five different solvents, viz., chloroform, methyl ethyl ketone (MEK), tetrahydrofuran (THF), isoamyl acetate and acetone (10% w/v) at room temperature. 4 phr (per hundred parts of rubber) of clay was then dispersed in six different solvents, viz., chloroform, MEK, THF, isoamyl acetate, acetone and ethanol (1 g in 50 ml) by sonicating in an ultrasonicator for 30 min at room temperature. Amount of clay was selected based on previous work done in our laboratory [13] and the solvents chosen have a range of solubility parameter. Along with other solvents, ethanol was chosen as a dispersing solvent based on the earlier work done by Sadhu and Bhowmick [14]. The

Table 1a
Solubility parameter of different solvents and their interaction parameter with rubber and clay.[a]

Solvent for rubber	Solvent for clay	δ[b] [(MPa)$^{1/2}$]	δ_D[b] [(MPa)$^{1/2}$]	δ_P[b] [(MPa)$^{1/2}$]	δ_H[b] [(MPa)$^{1/2}$]	H-bond	χ_{AB}[c]	χ_{CD}[c]
Isoamyl acetate	Isoamyl acetate	17.20	15.30	3.10	7.00	m	0.02	0.09
Chloroform	Chloroform	18.76	17.80	3.10	5.70	p	0.05	0.03
MEK	MEK	18.91	16.00	9.00	5.10	m	0.07	0.05
THF	THF	19.46	16.80	5.70	8.00	p	0.15	0.16
Acetone	Acetone	20.30	15.50	10.40	7.00	m	0.38	0.50
–	Ethanol	26.00	15.80	8.80	19.40	s	–	7.20

[a] Values of solubility parameter have been taken from Ref. [26].
[b] δ = Total solubility parameter; δ_D = component due to dispersion forces; δ_P = component due to polar forces; δ_H = component due to H-bonding.
[c] χ_{AB} and χ_{CD} are rubber–solvent and clay–solvent interaction parameters respectively and have been determined from Equations (7) and (8).

Table 1b
Name and designation of various solvent combinations used for preparation of HNBR nanocomposites.

Sl no.	Solvent for HNBR	Solvent for clay	Combination	Designation
1	Chloroform (Ch)	Chloroform (Ch)	HNBR in Ch/clay in Ch	Ch/Ch
2	Methyl ethyl ketone (MEK)	Methyl ethyl ketone (MEK)	HNBR in MEK/clay in MEK	MEK/MEK
3	Tetrahydrofuran (THF)	Tetrahydrofuran (THF)	HNBR in THF/clay in THF	THF/THF
4	Acetone (Ac)	Acetone (Ac)	HNBR in Ac/clay in Ac	Ac/Ac
5	Isoamyl acetate (IAAc)	Isoamyl acetate (IAAc)	HNBR in IAAc/clay IAAc	IAAc/IAAc
6	Chloroform (Ch)	MEK	HNBR in Ch/clay in MEK	Ch/MEK
7	Chloroform	Ethanol (Et)	HNBR in Ch/clay in Et	Ch/Et
8	THF	Ethanol (Et)	HNBR in THF/clay in Et	THF/Et
9	MEK	Ethanol (Et)	HNBR in MEK/clay in Et	MEK/Et

clay dispersion was then poured into the prepared rubber solution and stirred vigorously for 1 h at room temperature to make a homogenous mixture. The solution was finally cast on a Petri dish at 35 °C to get a thin film. The solvent was allowed to evaporate at room temperature and dried in a vacuum oven at 50 °C till there was no weight variation.

2.3. X-Ray Diffraction (XRD)

For the characterization of the rubber nanocomposites, XRD studies were performed using a PHILIPS X-PERT PRO diffractometer in the range of 2–9°(2θ) and Cu target ($\lambda = 0.154$ nm). Then, *d*-spacing of the clay particles was calculated using Bragg's law. The samples were placed vertically in front of the X-ray source.

2.4. Atomic Force Microscopy (AFM)

Multi Mode Scanning Probe Microscope model with a Nanoscope IIIa controller by Digital Instruments Inc. (Veeco Metrology Group), Santa Barbara, CA, USA, was used for the AFM studies. The AFM measurements were carried out in air at ambient conditions (25 °C), using tapping mode probes with constant amplitude (40 mV). The rotated tapping mode-etched silicone probe (RTESP) [square pyramid in shape with a spring constant of 20 N/m, nominal radius of curvature of 10 nm] with resonance frequency of 270 kHz was used. Height and phase images were recorded simultaneously at the resonance frequency of the cantilever with a scan rate of 1 Hz and a resolution of 512 samples per line. This allowed the resolution of individual primary particle measurements. The images were analyzed using a nanoscope image processing software (5.30r1).

2.5. Transmission Electron Microscopy (TEM)

The samples for TEM analysis were prepared by ultracryomicrotomy with a Leica Ultracut UCT (Leica Microsystems GmbH, Vienna, Austria). Freshly sharpened glass knives with cutting edges of 45° were used to obtain cryosections of about 100–150 nm thickness at −90 °C. The cryosections were collected individually in sucrose solution and directly supported on a copper grid of 300 mesh. Microscopy was performed with JEOL 2100, Japan. Transmission electron microscope was operated at an accelerating voltage of 200 kV.

2.6. Calculation of surface energy and solubility parameter of sepiolite

The surface energy of clay was determined by contact angle measurement [15]. A contact angle meter, Kernco (Model G II), was adopted for contact angle measurement, using water and formamide as the testing liquids.

The contact angle of the liquids (water and formamide) on clays was determined using Washburn equation [16].

$$\frac{w^2}{t} = \frac{c\gamma_1 \cos\theta {\rho_1}^2}{2\eta e} \tag{1}$$

where w is the mass of the penetrating liquid, γ_1 is the surface tension of the liquid used, θ is the contact angle of the liquid on the powder, ρ_1 is the density of liquid, t is the equilibrium time, η_e is the viscosity of the liquid, and c is the constant, which is a function of effective pore radius and another constant. Constant 'c' was measured using toluene for which $\theta = 0°$, i.e., $\cos\theta = 1$.

Surface energy of clay was estimated from the following equation [17]

$$\cos\theta = -1 + \frac{2(\gamma_S^d \gamma_l^d)^{1/2}}{\gamma_1} + \frac{2(\gamma_S^p \gamma_l^p)^{1/2}}{\gamma_1} \tag{2}$$

where γ_S^d and γ_S^p are the dispersion and polar components of solid's surface energy and γ_l^d and γ_l^p are the dispersion and polar components of liquid's surface energy. Hence, the surface energy of the solid,

$$\gamma_S = \gamma_S^d + \gamma_S^p \tag{3}$$

Based on Hilderbrand and Scott [18] solubility parameter and Hansen's work [19], Beerbower [20] proposed a relationship between surface energy and solubility parameter

$$\gamma_S = 0.07147\delta^2 V_i^{1/3} \tag{4}$$

where δ is the solubility parameter and V_i is the molar volume.

V_i can be expressed as

$$V_i = \frac{M_i}{\rho} \tag{5}$$

where M_i is the molar mass of the interacting element and ρ is the density of the substance.

From the knowledge of surface energy of clay as obtained from Equation (2), the solubility parameter of clay can be determined from Equation (4).

Using Equation (4), the solubility parameter of montmorillonite clay (Cloisite 15A) was found out [$\delta = 17.99$ (MPa)$^{1/2}$] to be identical with the literature value [7] and thus the method was justified.

2.7. Light transmittance

The specimen for the measurement of optical transmittance had a thickness of 2 mm. The light transmittance of the composite was measured within the wavelength range 200–400 mm^{-1} using an UV-1601, Visible Spectrometer (SHIMADZU), Japan.

2.8. Mechanical properties

Tensile specimens were punched out from the cast sheets using ASTM Die-C. The tests were carried out as per the ASTM D 412-98 method in a Universal Testing Machine (Zwick/Roell Z010) at a crosshead speed of 500 mm/min at 25 °C. The average of three tests is reported here. The error was ±2% in the measurements of tensile strength and modulus and ±5% for elongation at break.

2.9. Thermo Gravimetric Analysis (TGA)

Thermo Gravimetric Analysis was done using Perkin Elmer Instrument, Diamond TG-DTA. The samples (3–5 mg) were heated from ambient temperature to 800 °C in the furnace of the instrument under oxygen atmosphere at 100 ml/min and at a heating rate of 20 °C/min and the data of weight loss vs. temperature were recorded. Although the experiments were recorded in nitrogen as well as in air, there was major difference amongst the samples when oxygen was used as the medium. The analysis of the thermo gravimetric (TG) and derivative thermo gravimetric (DTG) curves was done in oxygen and the onset temperature, weight loss at major degradation steps and temperature corresponding to the maximum value in the derivative thermogram were recorded. The temperature at which maximum degradation took place is denoted as T_{max} and onset temperature of degradation is denoted as T_i. The error in the measurement was ±1 °C.

3. Results

The X-ray diffractograms of the sepiolite clay and HNBR–sepiolite nanocomposites in different solvent combinations are shown in Fig. 2. Both the clay and the nanocomposites have peak position in the range of 7.2–7.4°(2θ), corresponding to d-spacing of 1.22–1.24 nm. This indicates that unlike montmorillonite [21] which is a layered silicate, sepiolite clay does not undergo exfoliation on addition to the rubber matrix. In the case of smectite clays (e.g. MMT), "exfoliation" refers to the separation of platelets followed by dispersion of those platelets throughout the polymer matrix. No such exfoliation is, however, observed in the case of sepiolite clays, where unlike MMT, individual TOT (tetrahedral octahedral tetrahedral) layers are connected through covalent bond (Fig. 1) and the clay is fibrous in nature. Unlike smectite clays, here fiber bundles or aggregates get separated in nanometer dimension which are then dispersed/delaminated throughout the polymer matrix. Wang and Sheng [22] have made similar observations for polypropylene/attapulgite nanocomposite. Attapulgite (also called palygorskite) like sepiolite is a crystalline hydrated magnesium aluminium silicate and has a fibrous morphology.

Decrease in the peak intensity in the case of nanocomposite reveals that clay sheets get delaminated to a certain extent. Lower the intensity of peak, higher is the delamination. As in the case of HNBR in chloroform/clay in MEK combination, the peak intensity is the lowest; clay layers undergo maximum delamination in this solvent combination. AFM and TEM photographs described in the next section also confirm the above observations.

AFM photographs of rubber–clay nanocomposites in Ch/MEK and Ch/Et solvent system are shown in Figs. 3 and 4. Here in Ch/MEK system, nanoclays are dispersed uniformly, while in Ch/Et solvent combination, there is poor dispersion of the nanoclays in the rubber matrix, an example of homogenous and heterogeneous dispersion respectively. These photographs further reveal that average thickness of clay particles is 10–15 nm in Ch/MEK solvent combination (Fig. 3a), while clays form agglomeration in the case of Ch/Et solvent system having an average thickness of about 60–120 nm, as shown in Fig. 4a.

From Figs. 3 and 4, it is concluded that selection of perfect solvent combination acts as a precursor to the morphology generation of the nanocomposites.

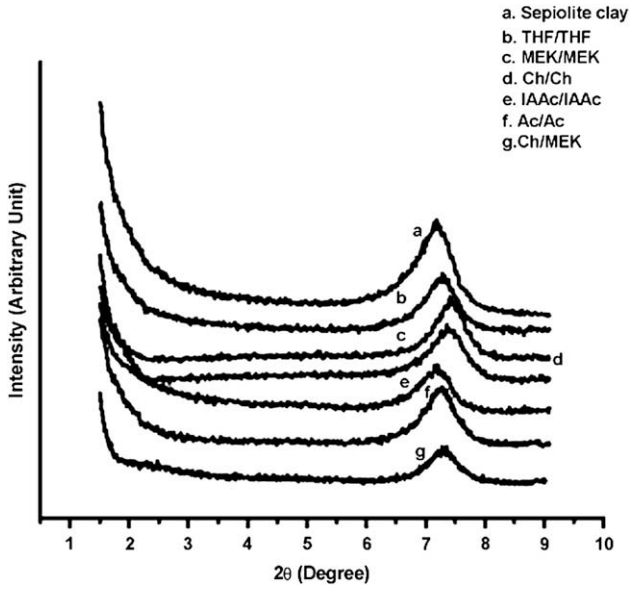

Fig. 2. XRD curves of sepiolite clay and HNBR–sepiolite nanocomposite for various solvent combinations.

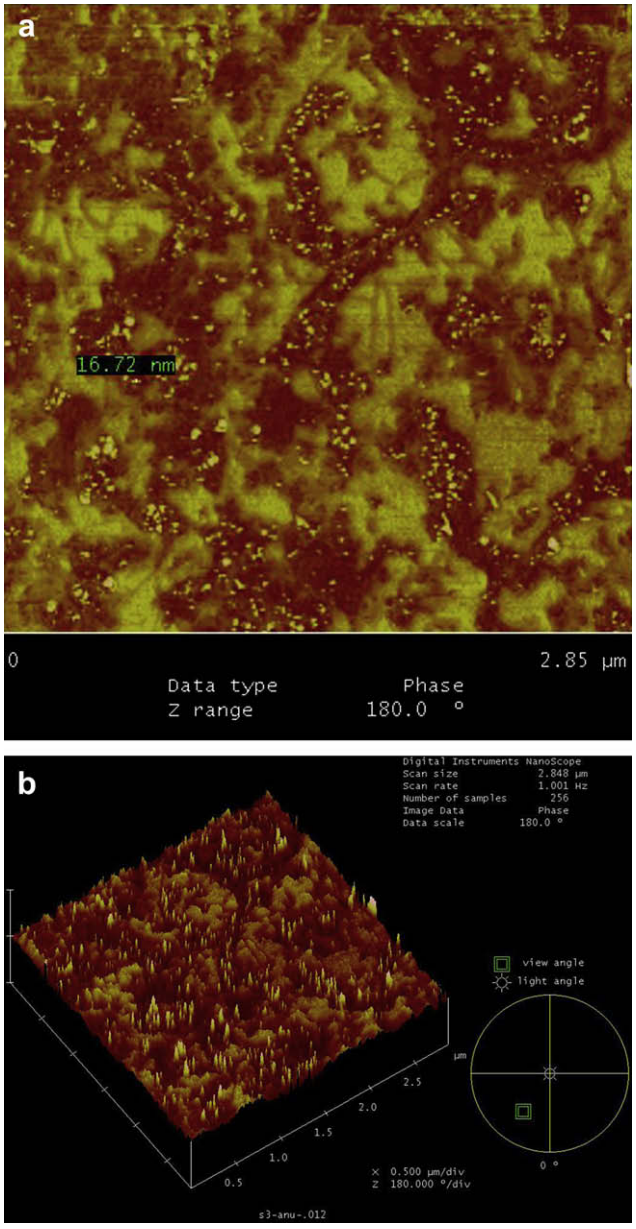

Fig. 3. (a) Phase image and (b) 3D image of HNBR–sepiolite nanocomposite for chloroform/MEK solvent combination.

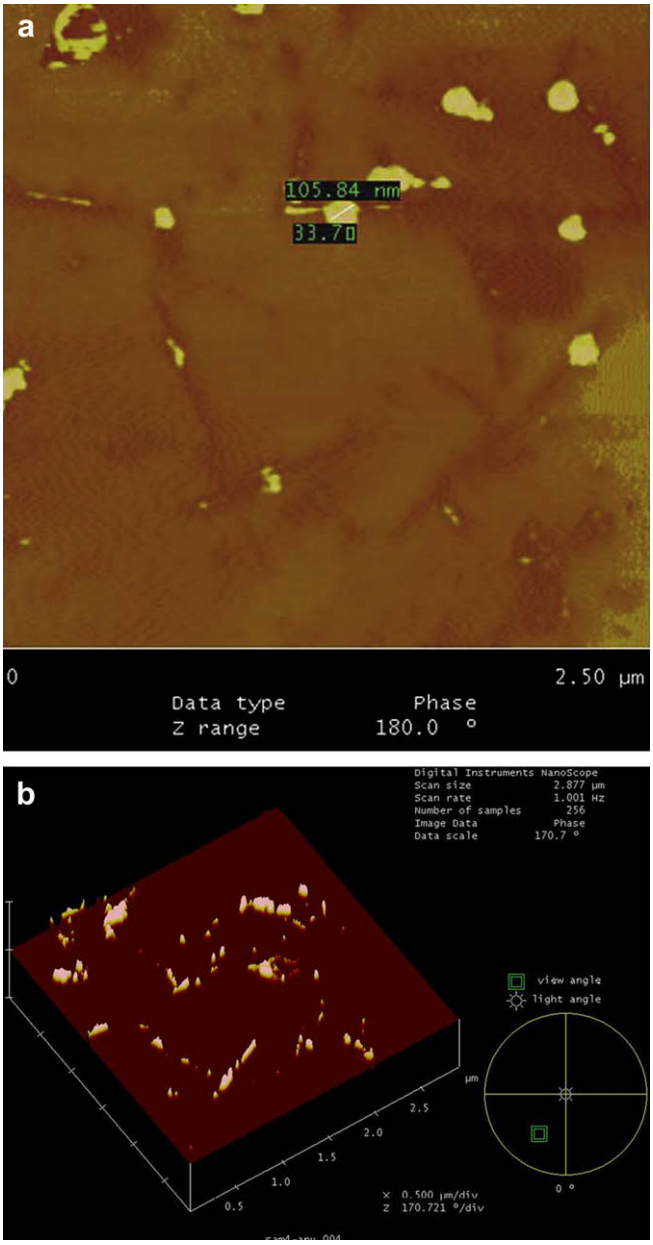

Fig. 4. (a) Phase image and (b) 3D image of HNBR–sepiolite nanocomposites for chloroform/ethanol solvent combination.

Also, TEM photograph (Fig. 5a and b) confirms the distribution of fibrous clay particles throughout the matrix for the nanocomposite prepared in chloroform/MEK solvent combination (Fig. 5a), while clay particles form agglomeration in the case of chloroform/ethanol solvent combination (Fig. 5b).

3.1. Optical property

Transparency is an important tool to understand the dispersion of clay in rubber matrix. Higher the transparency of the cast film made of rubber–clay nanocomposite, better is the dispersion of the clay in the rubber matrix. Transparency of HNBR–sepiolite nanocomposites for different solvent combinations, measured by ultraviolet spectroscopy at 325 mm^{-1}, is tabulated in Table 2.

Transparency value is highest for Ch/MEK solvent system (78%) followed by THF/THF (62%), Ch/Ch (55%), MEK/MEK (51%), IAAc/IAAc (48%), Ac/Ac(33%). Low transparency value indicates poor dispersion of the nanoclay in the rubber matrix. It might seem that the swollen (but not exfoliated) clay lumps would be larger in size and therefore more likely to scatter light. Deng et al. [23] have shown the effect of morphology on the optical properties of the epoxy–nanocomposite and have found that higher the transparency, better is the exfoliation of montmorillonite clay in the matrix, i.e., better dispersion.

3.2. Mechanical properties

Mechanical properties of rubber–clay nanocomposite cast from various solvent systems and the neat rubber are listed in Table 3. The modulus values at 100% elongation of the rubber–clay nanocomposites in Ch/MEK, THF/THF, MEK/MEK, Ch/Ch, IAAc/IAAc, Ac/Ac, THF/Et, MEK/Et and Ch/Et solvent combinations are 1.5, 1.2, 1.0, 1.0, 0.9, 0.8, 0.7, 0.7 and 0.6 MPa respectively. This indicates that the modulus increases by 200%, 140%, 100%, 100%, 80%, 60%, 40%, 40% and 20% for the above solvent combinations respectively. The tensile strength is also enhanced by 190%, 140%, 125%, 120%, 90%, 65%, 40%, 15% and 5% respectively. The elongation at break for all the samples is greater than 1600%. When the modulus of the nanocomposite is higher, the elongation at break reduces, in line with the conventional concept. Improved modulus and tensile strength of the nanocomposite in Ch/MEK solvent system indicate the fact that both the polymer–clay interaction and the dispersion of clay in the polymer matrix are best in such solvent combination. Thus, when HNBR is solubilized in chloroform and the sepiolite is dispersed in MEK, the nanocomposite exhibits the best modulus at 100% elongation and tensile strength.

Interestingly, it is observed from Table 3 that with the addition of only 4 parts of clay, modulus and tensile strength significantly increase. However, both the modulus at 100% elongation and the tensile strength are low for the HNBR–sepiolite nanocomposite, when sepiolite is dispersed in ethanol. The results could be explained with the help of solubility parameter difference between clay and ethanol, rubber–solvent and clay–solvent interaction parameter as explained later.

3.3. Thermal properties

T_{max} and T_i values of the neat HNBR and HNBR–clay nanocomposites are tabulated in Table 4 and DTG curves for nanocomposites in some selective solvent combinations are shown in Fig. 6. There are three degradation temperatures designated as T_{max1}, T_{max2} and T_{max3} for neat HNBR, one major corresponding to 421 °C (T_{max2}) and two minor at 404 °C (T_{max1}) and 437 °C (T_{max2}) in oxygen. For nanocomposites in Ch/MEK, THF/THF, IAAc/IAAc, Ac/Ac solvent combinations, one single degradation temperature corresponding to 486 °C, 478 °C, 462 °C and 455 °C respectively is observed (Table 4) and T_{max} value is shifted significantly for the nanocomposites prepared in various solvent combinations (65 °C in Ch/MEK, 57 °C in THF/THF, 55 °C in Ch/Ch, 54 °C in MEK/MEK, 41 °C in IAAc/IAAc, 34 °C in Ac/Ac, 31 °C in THF/Et, 30 °C in MEK/Et, 30 °C in Ch/Et). A similar trend is also observed with T_i, the onset temperature. For the neat HNBR, the onset of degradation is 400 °C. T_i for the nanocomposites is shifted by 46 °C, 36 °C, 33 °C, 30 °C, 27 °C, 26 °C, 25 °C, 23 °C, and 21 °C in Ch/MEK, THF/THF, Ch/Ch, MEK/MEK, IAAc/IAAc, Ac/Ac, THF/Et, MEK/Et and Ch/Et system respectively. Thus, both T_{max} and T_i values are highest for the system where clay is dispersed in MEK and rubber is dissolved in chloroform.

4. Discussion

From the above results, it can be summarized that HNBR–sepiolite nanocomposite provides the best thermal, optical and mechanical properties when HNBR is dissolved in chloroform and

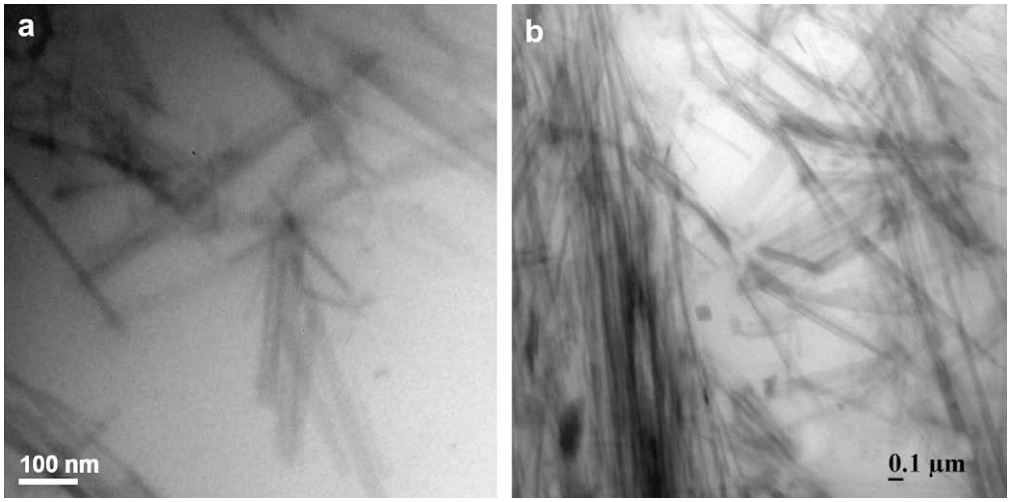

Fig. 5. TEM photograph of HNBR–sepiolite nanocomposite in (a) chloroform/MEK and (b) chloroform/ethanol solvent combination.

sepiolite is dispersed in methyl ethyl ketone (MEK). X-Ray Diffraction, Atomic Force Microscopy, Transmission Electron Microscopy and optical transmittance studies show that the dispersion of clay is best in the Ch/MEK solvent combination and hence polymer–filler interaction is also highest in this system. Thus rather than implying that the solvent selection directly affects the physical properties of the nanocomposite, solvent acts on the properties through its influence on the developed morphology. In order to understand the above results, we take recourse to solubility parameter and interaction parameter between various systems as listed in Table 1a.

Solubility parameter of the rubber, can be determined by Hoffman and van Krevelen additive group contribution method [24,25] as given by

$$\delta = \frac{\sum F_i}{V} \tag{6}$$

where $\sum F_i$ = the sum of the group contribution of all the chemical groups in the repeat unit. Values of F_i for a no. of groups are tabulated in Table 5 [26] and the solubility parameter of HNBR calculated from Equation (6) and that of sepiolite estimated from Equation (4) are represented in Table 6.

Knowing the solubility parameter of the rubber and the clay and from the knowledge of the solubility parameter of solvents as listed in Table 1a, the interaction parameter of rubber–solvent and clay–solvent can be determined from Hilderbrand solubility parameter [18] as

For rubber–solvent

$$\chi_{AB} = \frac{V_M}{RT}(\delta_a - \delta_b)^2 \tag{7}$$

Table 2
Transparency of the cast film of HNBR–sepiolite nanocomposite for various solvent combinations.

Sl no.	Solvent system	$\chi_{AB} - \chi_{CD}$	Transmittance (%) from UV
1	Ch/MEK	0.00	78
2	THF/THF	0.01	62
3	Ch/Ch	0.02	55
4	MEK/MEK	0.02	51
5	IAAc/IAAc	0.07	48
6	Ac/Ac	0.12	33
7	THF/Et	7.01	30
8	MEK/Et	7.11	28
9	Ch/Et	7.15	22

where V_M is the molar volume of solid segment, T is the absolute temperature and R is the gas constant.

Similarly, for clay–solvent

$$\chi_{CD} = \frac{V_M}{RT}(\delta_c - \delta_d)^2 \tag{8}$$

Interaction parameter between HNBR–solvent (χ_{AB}) and sepiolite–solvent (χ_{CD}) is calculated using Equations (7) and (8) and the values are reported in Table 1a.

From Equations (7) and (8), the difference in interaction parameters between rubber–solvent and clay–solvent ($\chi_{AB} - \chi_{CD} = \chi$) system has been calculated and the values are shown in Tables 2–4.

In order to understand the relationship of differences in interaction parameter of rubber–solvent (χ_{AB}) and clay–solvent (χ_{CD}) system, with the properties of HNBR–sepiolite nanocomposite, the plots of modulus at 100% elongation and tensile strength vs. $\chi_{AB} - \chi_{CD}$ are represented in Fig. 7a and b. Fig. 8a and b represents the plots of T_i and T_{max} vs. difference of interaction parameter ($\chi_{AB} - \chi_{CD}$), respectively. An exponential decay in both modulus and tensile strength is observed with the increase in difference of interaction parameter. T_i and T_{max} follow the same trend as above.

All the curves fit into the following second order exponential decay equation

$$y = A_1 * \exp\left(-\frac{x}{t_1}\right) + A_2 * \exp\left(-\frac{x}{t_1}\right) + y_0 \tag{9}$$

Exponential decay means decrease in the properties with increasing difference in interaction parameter that followed an exponential function. In Equation (9), y and x are two variables

Table 3
Mechanical properties of HNBR–sepiolite nanocomposite for various solvent combinations.

Sl no.	System	$\chi_{AB} - \chi_{CD}$	Modulus at 100% elongation (MPa)	Tensile strength (MPa)	EAB[a] (%)
1	Neat rubber	–	0.50	2.00	2400
2	Ch/MEK	0.00	1.50	5.90	1600
3	THF/THF	0.01	1.20	4.80	1800
4	Ch/Ch	0.02	1.00	4.50	1700
5	MEK/MEK	0.02	1.00	4.40	1600
6	IAAc/IAAc	0.07	0.85	3.80	1800
7	Ac/Ac	0.12	0.80	3.30	1800
8	THF/Et	7.01	0.70	2.80	2100
9	MEK/Et	7.11	0.65	2.30	1900
10	Ch/Et	7.15	0.63	2.10	2000

[a] EAB = elongation at break.

Table 4
Thermal properties of HNBR–sepiolite nanocomposite for various solvent combinations in oxygen atmosphere at 20 °C/min.

Sl no.	System	$\chi_{AB} - \chi_{CD}$	T_i (°C)	T_{max1} (°C)	T_{max2} (°C)	T_{max3} (°C)
1	Neat rubber	–	400	404	421	437
2	Ch/MEK	0	446	–	486	–
3	THF/THF	0.01	436	–	478	–
4	Ch/Ch	0.02	433	–	476	489
5	MEK/MEK	0.02	430	–	475	481
6	IAAc/IAAc	0.07	427	–	462	–
7	Ac/Ac	0.12	426	–	455	–
8	THF/Et	7.01	425	452	452	479
9	MEK/Et	7.11	423	–	451	470
10	Ch/Et	7.15	421	–	451	473

representing respectively the properties of nanocomposites and the difference in interaction parameters between polymer–solvent and clay–solvent, t_1 and t_2 are constants called decay constant. A_1 and A_2 are the two constant quantities respectively, while y_0 denotes offset that is the initial quantity at time $t = 0$.

For modulus vs. difference in interaction parameter curve,
$y_0 = 0.71$; $A_1 = 0.38$; $t_1 = 0.07$; $A_2 = 0.79$; $t_2 = 0.008$; regression coefficient = 0.99.

Similarly, for the tensile strength vs. difference in interaction parameter plot
$y_0 = 2.95$; $A_1 = 0.99$; $t_1 = 0.003$; $A_2 = 1.94$; $t_2 = 0.14$; regression coefficient = 0.99.

For T_{max} vs. difference in interaction parameter plot,
$y_0 = 444.39$; $A_1 = 3.59$; $t_1 = 0.0003$; $A_2 = 38.04$; $t_2 = 0.092$; regression coefficient = 0.99.

For T_i vs. difference in interaction parameter plot,
$y_0 = 423.51$; $A_1 = 16.77$; $t_1 = 0.048$; $A_2 = 0.96$; $t_2 = 0.001$; regression coefficient = 0.99.

The mechanical properties (tensile strength and modulus) are found to be maximum (5.89 MPa and 1.50 MPa respectively) for Ch/MEK system where the difference in interaction parameter ($\chi_{AB} - \chi_{CD}$) is lowest, i.e., zero. The tensile strength and modulus of rubber–clay nanocomposites gradually decrease as the difference

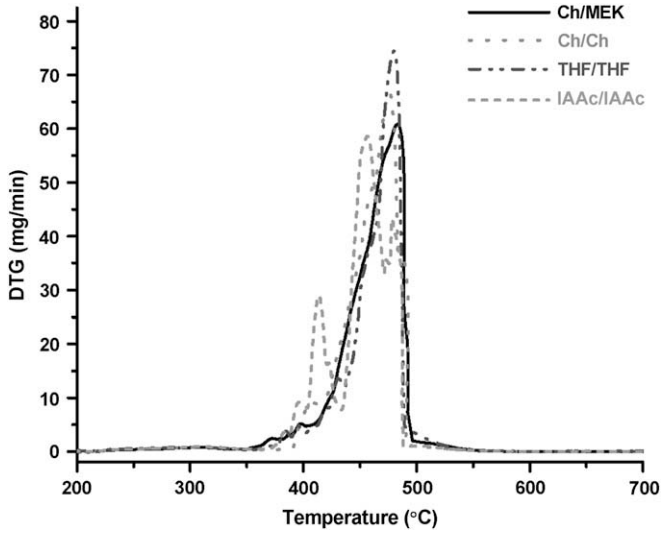

Fig. 6. DTG curves of HNBR–sepiolite nanocomposite for some selective solvent combinations.

Table 5
Values of F_i for various groups.

Group	F_i Value
$-CH_3$	437
$=CH_2$	272
$=CH-$	57
$-CN$	839

in interaction parameter ($\chi_{AB} - \chi_{CD}$) increases and these become lowest for Ch/Et solvent combination where $\chi_{AB} - \chi_{CD}$ is highest among nine solvent combinations. A similar trend is observed in the case of thermal property of HNBR–sepiolite nanocomposites. Both T_{max} and T_i are highest for Ch/MEK solvent combination and gradually decrease and become lowest for Ch/Et system.

The present work also establishes a correlation between the transmittance property of rubber–clay nanocomposites and the difference in interaction parameter ($\chi_{AB} - \chi_{CD}$), as shown in Fig. 9. This plot also follows the second order exponential decay and fit into the same Equation (9), with $y_0 = -2276.74$; $A_1 = 20.79$; $t_1 = 0.007$; $A_2 = 2334.15$; $t_2 = 12.32$; regression coefficient = 0.97.

The analysis of variance (ANOVA) of these data is given in Table 7.

The transmittance (%) is highest for Ch/MEK solvent system (78% as obtained from UV) and a decreasing trend is observed with increase in difference of interaction parameter ($\chi_{AB} - \chi_{CD}$).

Thus, among nine solvent systems studied here, dispersion of clay in rubber is most uniform in Ch/MEK solvent combination. Chloroform and MEK are two different solvents but having almost same solubility parameter as represented in Table 1a (18.76 and 18.91 respectively); hence they are thermodynamically miscible. The thermodynamic criteria of miscibility are based on the free energy of mixing ΔG_m. Two solvents are miscible with each other if ΔG_m is negative. By definition,

$$\Delta G_m = \Delta H_m - T\Delta S_m \tag{10}$$

where ΔH_m = enthalpy of mixing;
ΔS_m = entropy of mixing;
T = absolute temperature.

As ΔS_m is generally positive, there is certain limiting value of ΔH_m, below which dissolution is possible.

According to Hildebrand, the enthalpy of mixing can be related with solubility parameter as

$$\Delta H_m = \phi_1\phi_2(\delta_1 - \delta_2)^2 \tag{11}$$

where ϕ_1 and ϕ_2 = volume fraction of components 1 and 2.
δ_1 and δ_2 = solubility parameter of components 1 and 2.

Equation (11) predicts that $\Delta H_m = 0$ if $\delta_1 \approx \delta_2$; thus chloroform and MEK having similar solubility parameters are miscible with each other. On the other hand, Ch/Et, THF/Et and MEK/Et are not thermodynamically favorable systems, as $|\delta_1 - \delta_2|$ is quite large for such type of systems (Table 1a).

Taken into account of three components of solubility parameter, δ_d, δ_p and δ_h of various solvents, as listed in Table 1a, dispersion of clay is always better in more polar solvent. Higher the polarity of

Table 6
Solubility parameter of rubber and clay.

Material	Solubility parameter $[(MPa)]^{1/2}$
HNBR	17.90
Sepiolite	18.30

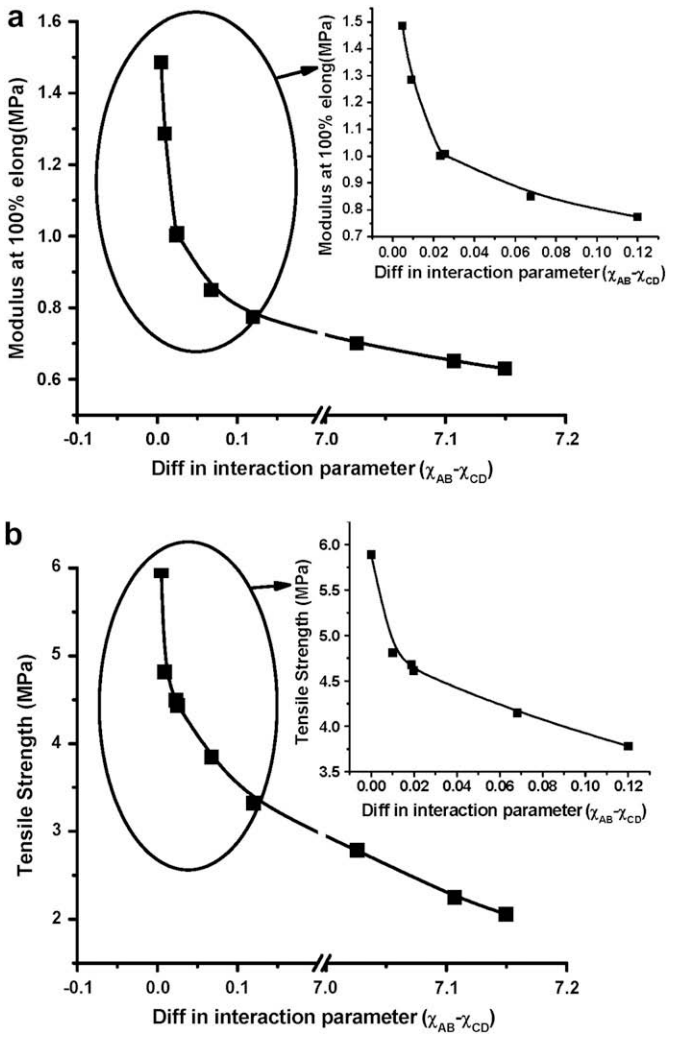

Fig. 7. Plot of (a) modulus at 100% elongation and (b) tensile strength vs. difference in interaction parameter ($\chi_{AB} - \chi_{CD}$).

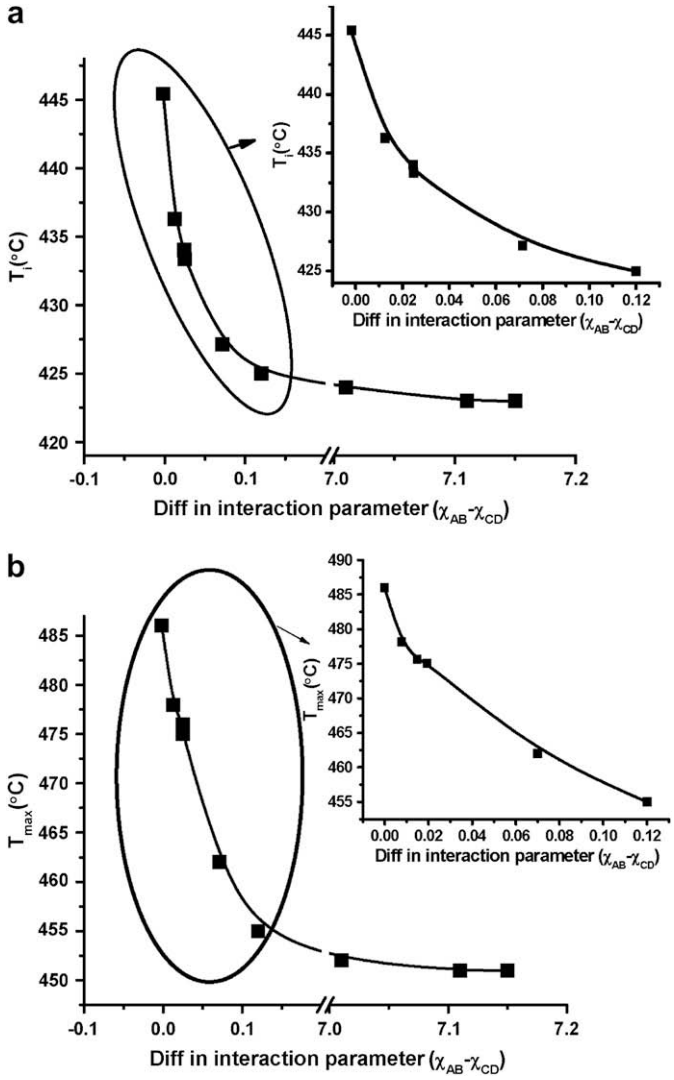

Fig. 8. Plot of (a) T_i and (b) T_{max} vs. difference in interaction parameter ($\chi_{AB} - \chi_{CD}$).

solvent, better will be the dispersion of clay. As sepiolite is polar clay, the extent of solvent penetration within the clay layers increases with polarity of the solvent. Since MEK has higher δ_p value in comparison to isoamyl acetate, THF and chloroform, the extent of dispersion of clay is better in MEK than the other three solvents. Acetone has higher δ_p value than that of MEK, but its higher value of $\chi_{AB} - \chi_{CD}$ in Ac/Ac combination (0.12) leads to inferior thermal, mechanical and optical properties of the nanocomposite. Hence, smaller the $\chi_{AB} - \chi_{CD}$ value, the better is the miscibility between the components and polymer–clay interaction, giving rise to better thermal, mechanical and optical properties as represented in Tables 2–4 and Figs. 7–9.

Better dispersion of clay as well as good polymer–filler interaction in the case of Ch/MEK solvent combination can also be predicted from thermodynamic point of view.

Gibb's free energy ΔG_M for mixing a solid with a solvent is

$$\Delta G_M = \Delta H_M - T\Delta S_M \quad (12)$$

where ΔH_M and ΔS_M are the enthalpy and entropy increments associated with the mixing process.

In a system there are three types molecular interaction to consider-solvent–solvent w_{11}, solid–solvent w_{12} and solid–solid w_{22}. Solid–solid interaction means interaction between different chain sections of the polymer or clay units or polymer–clay units.

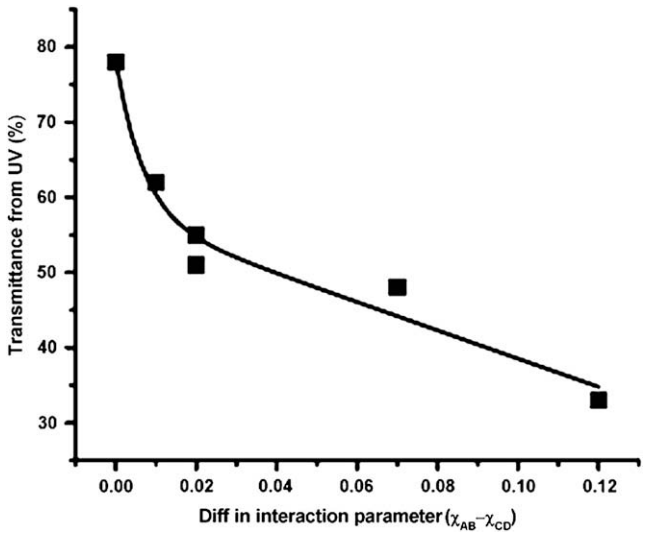

Fig. 9. Optical property of HNBR–sepiolite nanocomposite for various solvent combinations [% transmittance from UV vs. ($\chi_{AB} - \chi_{CD}$)].

Table 7
Analysis of variance (ANOVA) of various properties.

Properties	Source	DoF[a]	Sum of squares	Mean square	F[b] Value	P[c] Value	Remarks
Modulus at 100% elongation (MPa)	Model error	2	0.02	0.01	0.05	0.95	At the level of 0.05 the population means
		15	2.85	0.19			are not significantly different
Tensile strength (MPa)	Model error	2	0.04	0.02	0.03	0.97	At the level of 0.05 the population means
		15	12.50	0.84			are not significantly different
T_{max} (°C)	Model error	2	1.78	0.89	0.007	0.99	At the level of 0.05 the population means
		15	1984.50	132.30			are not significantly different
T_i (°C)	Model error	2	0.78	0.39	0.007	0.99	At the level of 0.05 the population means
		15	769.50	51.31			are not significantly different
Transmittance (%)	Model error	2	1.44	0.72	0.003	0.99	At the level of 0.05 the population means
		15	3515.66	234.37			are not significantly different

[a] Degree of freedom.
[b] Variance due to factor/variance due to error.
[c] Population means.

So, the energy increment per solid–solvent contact is

$$\Delta W = w_{12} - \frac{1}{2}(w_{22} + w_{11}) \tag{13}$$

Total number of such contact is

$$xN_2Z\phi_1 = N_1\phi_1 Z \tag{14}$$

where Z = coordination number, the number of nearest neighbor for a lattice site, each one occupied either by one solid molecule or a solvent molecule.
N_1 = Total number of solvent molecules;
N_2 = Total number of solid molecules each of which has x sheets/segments
xN_2 = Total number of polymer segments (monomers) or clay sheets.
xN_2Z = Total number of nearest neighbor sites of the solid.
ϕ_1 = volume fraction of the solvent.
ϕ_2 = volume fraction of the monomer segment or clay particle.

R.H. S. of Equation (14) implies total number of solid–solvent interacting sites.

Now, the enthalpy change is equal to the energy change (ΔW) per solid–solvent interaction multiplied by the no. of such interaction.

$$\Delta H_M = N_1\phi_2 Z\Delta W \tag{15}$$

Solid–solvent interaction parameter χ is defined as

$$\chi = \frac{Z\Delta W}{kT} \tag{16}$$

where k is Boltzmann's constant and T is the absolute temperature.

Interaction parameter χ is the energy of interdispersing solid molecules in solvent molecules. Lower is the energy, better is the dispersion or interaction of solid in solvent.

So, the enthalpy change (from Equations (15) and (16) becomes

$$\Delta H_M = kTN_1\phi_2\chi \tag{17}$$

Comparing Equations (12) and (17), Gibb's free energy ΔG_M can be represented as

$$\Delta G_M = kTN_1\phi_2\chi - T\Delta S_M \tag{18}$$

Equation (18) is true for both polymer–solvent and clay–solvent systems.

It is a well-known fact that lower the ΔG_M value, better is the rubber–filler interaction. As for Ch/MEK solvent combination χ is zero, hence $kTN_1\phi_2\chi$ term of Equation (18) is zero for such a solvent combination. In all other solvent combination, where $\chi \neq 0$; $kTN_1\phi_2\chi$ term of equation (18) is positive. Thus ΔG_M of the system for Ch/MEK solvent combination is the least and rubber–filler interaction for such a solvent combination is most favorable.

Again, entropy of mixing (ΔS_M) signifies the increase in the uncertainty about the locations of the molecules when they are interspersed. This entropy change must be positive since there exists a high uncertainty about the spatial locations of the molecules when either the polymer and solvent or the clay and solvent are mixed. So, ΔG_M of Equation (18) is negative when entropy of the system is positive. From XRD, AFM and TEM, we have found that in the case of Ch/MEK solvent combination maximum delamination of the clay layers takes place. So, entropy change of the system for such a solvent combination is more positive and free energy change should be more negative.

Thus finally, we can say that mixing of sepiolite with HNBR is always more favorable in Ch/MEK solvent combination.

5. Conclusion

HNBR–sepiolite nanocomposite was prepared by solution mixing using nine sets of solvent combination. In solution mixing process, the properties of polymer–clay nanocomposite are functions of difference in interaction parameter between rubber–solvent and clay–solvent. Chloroform/methyl ethyl ketone solvent system, where difference in rubber–solvent and clay–solvent interaction parameter is lowest, i.e., zero, thermal, mechanical and optical properties of HNBR–sepiolite nanocomposite are found to be the best. A thermodynamic interpretation has been made.

Acknowledgement

The authors are indebted to LANXESS, Germany for funding the project at IIT Kharagpur.

References

[1] Shen Z, Simon GP, Cheng YB. Polymer 2002;43(15):4251–60.
[2] Liang Y, Wang Y, Wu Y, Lu Y, Zhang H, Zhang L. Polym Test 2004;24(1):12–7.
[3] Strawhecker K, Manias E. Chem Mater 2000;12(10):2943–9.
[4] Plummer CJG, Garamszegi L, Leterrier Y, Rodlert M, Manson JE. Chem Mater 2002;14(2):486–8.
[5] Sur GS, Sun HL, Lyu SG, Mark JE. Polymer 2001;42(24):9783–9.
[6] Malwitz MM, Lin-Gibson S, Hobbie EK, Butler PD, Schmidt G. J Polym Sci Part B Polym Phys 2003;41(24):3237–48.
[7] Ho DL, Glinka CJ. Chem Mater 2003;15(6):1309–12.
[8] Liu J, Liu T, Kumar S. Polymer 2005;46(10):3419–24.
[9] Lift SM, Kumar N, McKinley GH. Nat Mater 2007;6:76–83.
[10] Lim SK, Kim JW, Chin I, Kwon YK, Choi HJ. Chem Mater 2002;14(5):1989–94.
[11] Duquesne E, Moins S, Alexandre M, Dubois P. Macromol Chem Phys 2007;208(23):2542–50.
[12] Bokobza L, Chauvin JP. Polymer 2005;46(12):4144–51.
[13] Maiti M, Sadhu S, Bhowmick AK. J Polym Sci Part B Polym Phys 2004; 42(24):4489–502.
[14] Sadhu S, Bhowmick AK. Rubber Chem Technol 2003;76(4):0860–75.

[15] Fowkes FM. In: Patrick RL, editor. Treatise on adhesion and adhesives, vol. 6. New York: Marcel Dekker; 1967. p. 1.
[16] Inagaki N, Tasaka S, Abe H. J Appl Polym Sci 1992;46(4):595–601.
[17] Bhowmick AK, Konar J, Kole S, Narayanan S. J Appl Polym Sci 1995;57(5): 631–7.
[18] Hilderbrand JH, Scott RL. The solubility of non-electrolyte. New York: Reinhold; 1950. p. 488.
[19] Hansen CM. J Paint Technol 1967;39(505):104–17.
[20] Beerbower A. J Colloid Interface Sci 1971;35(1):126–32.
[21] Maiti M, Bhowmick AK. J Polym Sci Part B Polym Phys 2006;44(1): 162–76.
[22] Wang L, Sheng J. Polymer 2005;46(16):6243–8.
[23] Deng Y, Gu A, Fang Z. Polym Int 2004;53(1):85–91.
[24] van Krevelen DW. Properties of polymer. 3rd ed., vol. 62. New York: Elsevier Amsterdam; 1990. p. 875.
[25] Hoffman RL. J Colloid Interface Sci 1975;50(2):228–41.
[26] Brandrup J, Immergut EH. Polymer handbook. 3rd ed. New York: Willey Interscience; 1989. p. VII/519.